



UNIVERSITY OF LEEDS

This is a repository copy of *Graphene-oxide-supported CuAl and CoAl layered double hydroxides as enhanced catalysts for carbon-carbon coupling via Ullmann reaction*.

White Rose Research Online URL for this paper:  
<http://eprints.whiterose.ac.uk/109086/>

Version: Accepted Version

---

**Article:**

Ahmed, NS, Menzel, R, Wang, Y et al. (5 more authors) (2017) Graphene-oxide-supported CuAl and CoAl layered double hydroxides as enhanced catalysts for carbon-carbon coupling via Ullmann reaction. *Journal of Solid State Chemistry*, 246. pp. 130-137. ISSN 0022-4596

<https://doi.org/10.1016/j.jssc.2016.11.024>

---

© 2016, Elsevier. Licensed under the Creative Commons Attribution-NonCommercial-NoDerivatives 4.0 International  
<http://creativecommons.org/licenses/by-nc-nd/4.0/>

**Reuse**

Unless indicated otherwise, fulltext items are protected by copyright with all rights reserved. The copyright exception in section 29 of the Copyright, Designs and Patents Act 1988 allows the making of a single copy solely for the purpose of non-commercial research or private study within the limits of fair dealing. The publisher or other rights-holder may allow further reproduction and re-use of this version - refer to the White Rose Research Online record for this item. Where records identify the publisher as the copyright holder, users can verify any specific terms of use on the publisher's website.

**Takedown**

If you consider content in White Rose Research Online to be in breach of UK law, please notify us by emailing [eprints@whiterose.ac.uk](mailto:eprints@whiterose.ac.uk) including the URL of the record and the reason for the withdrawal request.



[eprints@whiterose.ac.uk](mailto:eprints@whiterose.ac.uk)  
<https://eprints.whiterose.ac.uk/>

# Graphene-oxide-supported CuAl and CoAl layered double hydroxides as enhanced catalysts for carbon-carbon coupling via Ullmann reaction

Nesreen. S. Ahmed<sup>a, b</sup> Robert Menzel<sup>c, d</sup>, Yifan Wang<sup>c</sup>, , Ainara Garcia-Gallastegui<sup>d</sup>, Salem M. Bawaked<sup>a, b</sup>, Abdullah Y. Obaid<sup>a, b</sup>, Sulaiman N. Basahel<sup>a, b</sup>, Mohamed Mokhtar<sup>a, b\*</sup>

<sup>a</sup> Department of Chemistry, Faculty of Science, King Abdulaziz University, Saudi Arabia

<sup>b</sup> Surface Chemistry and Catalytic Studies Group, King Abdulaziz University, Saudi Arabia

<sup>c</sup> Department of Chemistry, Imperial College London, South Kensington Campus, London, SW7 2AZ, UK

<sup>d</sup> Bio Nano Consulting, The Gridiron Building, One Pancras Square, London, N1C 4AG, UK

\*Mohamed Mokhtar; Email: mmokhtar2000@yahoo.com

---

## Abstract

Two efficient catalyst based on CuAl and CoAl layered double hydroxides (LDHs) supported on graphene oxide (GO) for the carbon-carbon coupling (Classic Ullmann Homocoupling Reaction) are reported. The pure and hybrid materials were synthesised by direct precipitation of the LDH nanoparticles onto GO, followed by a chemical, structural and physical characterization by electron microscopy, X-ray diffraction (XRD), thermogravimetric analysis (TGA), surface area measurements, X-ray photoelectron spectroscopy (XPS) and temperature programmed reduction (TPR). The GO-supported and unsupported CuAl-LDH and CoAl-LDH hybrids were tested over the Classic Ullman Homocoupling Reaction of iodobenzene. In the current study CuAl- and CoAl-LDHs have shown excellent yields (91% and 98%, respectively) at very short reaction times (25 min). GO provides a light-weight, charge complementary and two-dimensional material that interacts effectively with the 2D LDHs, in turn enhancing the stability of LDH. As a result, the recyclability of the heterogeneous catalyst systems is greatly enhanced. After 5 re-use cycles, the catalytic activity of the LDH/GO hybrid is up to 2 times higher than for the unsupported LDH.

Keywords: Layered double hydroxide(s); graphine oxide; Ullmann Homocouplig Reaction.

---

## 1. Introduction

LDH-based materials display great potential as heterogeneous catalyst due to their versatility given by the possibility of incorporation of various catalytically-active transition metal species (e.g., Cu, Co, Fe, Ni, V, Rh), the strong alkaline nature and an easy separation of the products [1-3]. In particular, LDHs have been intensively investigated in recent years as catalysts and catalyst supports [4, 5] in many aspects, such as organic synthesis, (photo) degradation of organic wastes, greenhouse gas control emission and H<sub>2</sub> production [6-13].

However, the catalytic activity of LDHs is always limited by their tendency to aggregate and poor mechanical properties. Various methods have been explored to overcome these problems, such as the combination of LDH with carbon nanofibers [14] and carbon nanotubes [15-20], as previously studied in our group [21]. Among the nanocarbons, the 2D geometry of graphene oxide (GO) is obviously compatible with the layered structure of LDHs and there is also a charge compatibility between the positively charged LDH and negatively charged GO. The large

size of GO sheets compared to LDH platelets implies that it may be possible to form an open network with large pores allowing access of the reactants to the active LDH sites which is helpful for the high rate conversion of the reactants [15]. When combining LDH with GO, the heat and mass transfers during a reaction can be greatly improved. As previously observed in our group [22] GO can also offer the mechanical strength that allows a better stability of the catalyst under operation conditions, as well as facilitate the recovery and reuse of the catalyst. In this regard, there is one previous study that combines LDH and GO as heterogeneous catalyst and probes the enhancement of the catalytic activity mainly attributed to the higher metal dispersion and smaller size of deposited nanoparticles [23].

Among the catalytic reactions currently under study, the production of biaryl compounds have gained importance in the last decade [24-31]. The molecules containing this framework have shown activity across a wide range of therapeutic applications, which include antifungal, anti-inflammatory, antirheumatic, antitumor, and antihypertensive agents [32]. The main method for the synthesis of biaryls is the Classic Ullmann Homocoupling Reaction [33] based on the transition metal-catalyzed cross-coupling reaction starting from two discrete aromatic halide entities and stoichiometric amounts of organometallic reagents, originally copper [30, 34-39]. In principle, this reaction requires harsh reaction conditions, such as large excess of phenols, high temperatures (>200 °C) and at least stoichiometric amounts of copper, which result in the production of undesirable chemical waste [40]. Besides, most of the Cu based catalysts need an extra base and/or require long reaction times [41, 42]. As an alternative palladium, gold and nickel based catalysts have been introduced [43-46]. However, the metal catalyst together with the required ligands are expensive (Pd and Au) or even toxic (Ni), and above, they require an additional reducing agent, thus limiting their relevance for industrial applications.

Hence, it is of great practical interest to develop an efficient, inexpensive, solid heterogeneous catalyst that can catalyse the Ullmann coupling of aryls to biaryls in the absence of base, with short reaction time for a desirable product yield, which can be easily separated and reused in the reaction several times. Some attempts using different Cu catalysts systems have been reported [37, 47] and although the reaction yields can be high, unfortunately hours long completion times make the process impracticable. In an attempt to shorten the reaction time, our group has previously reported [48] microwave induced organic reaction enhancement over the Classic Ullmann Reaction to give biphenyl groups using Cu-Al LDH and reached a conversion of 91% at 120°C with a reaction completion time of 12 min. From a practical point of view, the aim in this work is to prepare catalysts that reach high yields in short completion time just applying temperature and avoiding any extra features such as the use of microwaves.

As an alternative to the classic copper-based Ullmann catalyst systems, cobalt-based LDH materials are also investigated. Cobalt has been extensively used for cross coupling reactions but only a handful of homocoupling reactions with good selectivity have been reported and all of them using substituted benzylic Grignard reagents [49]. It was not until 45 years later when Gosmini described good yields in the formation of unsymmetrical biaryls first [50, 51] and symmetrical biaryls later [52] both catalysed by cobalt in combination with manganese dust as reducing agent. When substituting phenyl groups by an electron withdrawing group yields of up to 84% have been reported. However, the product of this reaction is a substituted biaryl. When running the Classic Ullmann Reaction of homocoupling of iodobenzene to give the unsubstituted biaryl, the desired motif, scaffold of many therapeutic molecules [32] and our main focus here, the reported yield reached only 32 %. Recently Wangelin et al. [53] showed yields of up to 86 % using substituted benzylic Grignard reagents to give pure unsubstituted biaryls with reaction completion times as short as 30 min; yet the experimental procedure requires a purge of synthetic air as oxidant. Some other attempts have been published by Yu et al. [54] giving yields up to 81% using bromobenzene, Grignard reagents and atmospheric oxygen as oxidant but the reported completion time of 3 hours is still long from a practical point of view.

In order to improve further the catalyst and motivated by the aforementioned findings, in this study LDH materials were supported on Graphene Oxide (GO). Two hybrid materials with different LDH compositions were prepared, CuAl LDH/GO and CoAl LDH/GO, by in situ coprecipitation of LDH onto GO, in aqueous solution. The hybrids were fully characterised and their catalytic efficiency over the Classic Ullman Reaction was studied.

## 2. Experimental

2.1. Materials. Aluminium nitrate nonahydrate ( $\text{Al}(\text{NO}_3)_3 \cdot 9\text{H}_2\text{O}$ ), Copper nitrate trihydrate ( $\text{Cu}(\text{NO}_3)_2 \cdot 3\text{H}_2\text{O}$ ), Cobalt chloride hexahydrate ( $\text{CoCl}_2 \cdot 6\text{H}_2\text{O}$ ), Aluminium chloride hexahydrate ( $\text{AlCl}_3 \cdot 6\text{H}_2\text{O}$ ), and urea were

purchased from Sigma-Aldrich and used without further purification. NaOH, Na<sub>2</sub>CO<sub>3</sub> were purchased from AnalaR. Graphene oxide solution (10 mg mL<sup>-1</sup>) was purchased from ACSMaterial and used without further processing.

**2.2 Synthesis.** Cu-Al LDHs (Cu:Al ratio 2:1) were synthesised by co-precipitation at constant pH (pH=10) [48]. The reaction was carried out within an autotitrator system (Mettler Toledo T50 Titrator) in order to monitor and adjust pH. Using a syringe pump, an aqueous metal salt solution (24 mL, 0.67 M Cu(NO<sub>3</sub>)<sub>2</sub>•3H<sub>2</sub>O and 0.33 M Al(NO<sub>3</sub>)<sub>3</sub>•9H<sub>2</sub>O) was slowly added into an aqueous reservoir (100 mL, 0.01 M NaOH, pH 12) at 50°C at 25 mL h<sup>-1</sup>, using the overhead stirrer of the autoclave to ensure efficient fast mixing. An aqueous base solution (1 M NaOH, 1 M Na<sub>2</sub>CO<sub>3</sub>) was simultaneously added through the autotitrator to maintain a constant pH of 10. The resulting blue suspension was aged at 50°C for 20 h under stirring. The product was filtered using polycarbonate membranes (pore size 400 nm) and washed with HPLC water several times until the final pH reached 7. The precipitate was dried overnight at 80 °C. For the synthesis of the CuAl-LDH/GO hybrids (nominal LDH:GO ratio 20:1) **has been used, proven to be the optimal ratio in previous studies in our group [22]**, an aqueous GO dispersion (10 mL, 10 mg mL<sup>-1</sup>) was added to the initial aqueous reservoir, and the pH readjusted to pH 12. The co-precipitation, aging and washing procedures were carried out as described above.

CoAl LDHs (Co:Al ratio 2:1) were synthesised via a urea-mediated co-precipitation approach [55]. A dilute metal salt solution containing urea (400 mL; 10 mM CoCl<sub>2</sub>•6H<sub>2</sub>O, 5mM AlCl<sub>3</sub>•6H<sub>2</sub>O and 35 mM urea) was refluxed in nitrogen atmosphere at 97 °C under continuous magnetic stirring for 48 hours. The resulting pink precipitate was filtered, washed with HPLC water and ethanol several times until the final pH was 7, and dried overnight at 30°C. For the synthesis of the CoAl-LDH / GO hybrids (nominal LDH:GO ratio 20:1), an aqueous GO dispersion (2.5 mL, 10 mg mL<sup>-1</sup>) was added to the metal salt solution, while the rest of the synthesis and washing procedures remained the same.

**2.3. Catalytic test.** The catalyst (0.25 g), iodobenzene (2.0 mmol), and DMSO (4.0 mL) were mixed in a three necked round bottomed flask. The reaction mixture was heated at 110°C in a thermostatic oil-bath for the required time to complete the reaction as monitored by TLC. The progress of the reaction was monitored by thin layer chromatography (TLC) for every 5 min (eluent; petroleum ether: chloroform). After the completion of the reaction, the reaction mixture was cooled to room temperature and the catalyst was removed by filtration, washed with CHCl<sub>3</sub> and the solvent was evaporated under reduced pressure to obtain the product.

**2.4. Material Characterisation.** X-ray diffraction (XRD) measurements were performed using a PANalytical X'Pert Pro Multi Purpose Diffractometer (Cu K $\alpha$  radiation) in reflection mode at room temperature, between 5° to 80°. Scanning electron microscopy (SEM) images were taken using Gemini 1525 FEGSEM. Transmission electron microscopy (TEM) images were taken by a JOEL 2010, operating at 200 kV. Thermogravimetric analysis (TGA) was carried out using a PerkinElmer Pyris 1 Thermogravimetric Analyser. The samples (10  $\pm$  1 mg ) were first dried at 100°C for 60 min under N<sub>2</sub> and then heated from 100°C to 850 °C at 10 °C min<sup>-1</sup> in air (20 mL min<sup>-1</sup>). For Brunauer-Emmett-Teller (BET) measurements, samples (100 mg) were pre-dried overnight under N<sub>2</sub> at 40°C prior to the measurements. N<sub>2</sub> adsorption and desorption isotherms were measured at 77 K using a Micromeritics TriStar 3000 apparatus. Surface areas were calculated according to the BET equation. The mesopore volume and the mesopore size distribution were calculated from the desorption branch of the sorption isotherm via Barnett-Joyner-Halendar (BJH) analysis. XPS spectra of powdered graphite samples were recorded using a Thermo Scientific K-Alpha instrument using focused (400 mm spot) monochromatic Al-K $\alpha$  radiation at a pass energy of 40 eV. The binding energies were referenced to the C 1s peak of adventitious carbon at 284.8 eV. Temperature programmed reduction (TPR) was carried out, using a Micromeritics AUTOCHEM 2920 apparatus. Prior to the analysis, the untreated samples (20-40 mg) were preconditioned at 110°C for 2 hours under helium. Subsequently, the atmosphere was switched to 10% H<sub>2</sub> in Argon (50 mL.min<sup>-1</sup>) and the sample was heated up to 900°C at 10°C.min<sup>-1</sup>. The gases evolved were monitored via a thermal conductivity detector. In order to avoid interference, formed water was condensed in an iso-propanol bath (-40°C), located between the sample and the detector. All melting points of the products were measured on a Gallenkamp melting point apparatus and are uncorrected. The infrared spectra were recorded in KBr disks on Shimadzu FTIR 8101 PC infrared spectrophotometers. The NMR spectra were recorded on a Var-ian Mercury VX-300 NMR spectrometer. <sup>1</sup>H spectra were run at 300 MHz in CDCl<sub>3</sub>. Chemical shifts were related to that of the solvent. GC-MS analysis was carried out using Shimadzu, GCM-SQP2010S

equipped with a direct insertion probe (DIP) was used to acquire the mass spectra of extracted volatile organic compounds and detected in the electron impact mode (EI-MS) by the application of 70 eV as the ionization energy.

### 3. Results and Discussion

Electron microscopy (Figure 1 and Figure 2) was carried out to investigate the morphology of the synthesised LDH catalysts.

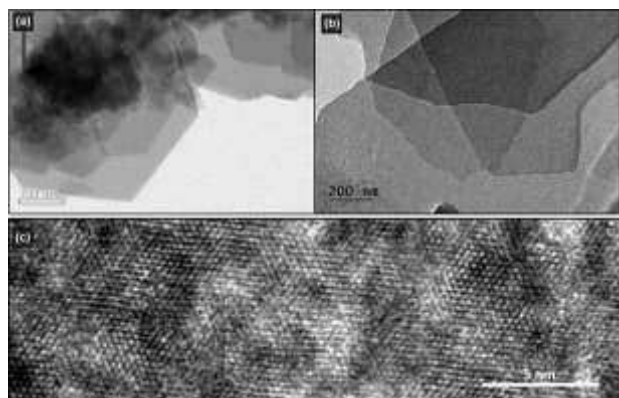


Fig. 1. TEM images of LDH catalyst particles: (a) Cu-Al LDH; (b) Co-Al LDH; (c) high resolution TEM of Co-Al LDH.

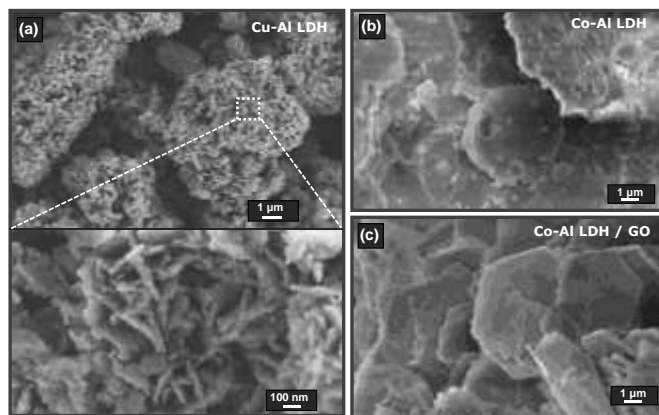


Fig. 2. SEM images of pure and GO-containing LDH catalysts: (a) Cu-Al LDH/GO; (b) Co-Al LDH; (c) Co-Al LDH / GO.

Both TEM and SEM showed CuAl-LDH particles with lateral particle sizes of several 100 nanometers (Figure 1a) while the individual CoAl-LDH particles are considerably larger, with lateral particle dimensions of up to 8  $\mu\text{m}$  (Figure 2b). SEM imaging (Figure 2) clearly showed that the individual CuAl- and CoAl-LDH particles cluster together into larger aggregates while TEM confirmed the crystallinity and typical hexagonal, platelet-like shape of the individual CuAl- and CoAl-LDH nanoparticles. For the GO-supported CuAl-LDH and CoAl-LDH materials (Figures 2a and 2c), SEM indicated similar individual particle sizes as observed for the pure LDH catalysts. Further, SEM fails to visualize any indication for GO in the hybrids, suggesting the presence of well-exfoliated GO sheets, fully covered by LDH particles. It is worth noting however that the packing of the individual hexagonal LDH particles within CoAl-LDH/GO sample (Figure 2c) appeared relatively loose and random compared to the dense and aligned packing in the

pure CoAl-LDH particles (Figure 2b), suggesting the presence of GO in the interstitial spaces of the hybrid material.

TGA under oxidative conditions was carried out to confirm the presence of GO in the hybrid materials (Figure 3). All LDH samples exhibited two distinct stages of weight loss upon temperature increase, the first stage (around 240°C) related to the loss of crystal water while the second stage (at 650°C for CuAl-LDH and at 300° for CoAl-LDH) related to the release of intercalated anions. The actual GO weight percentage in the sample can be estimated from the TGA residues. The smaller TGA residue weight of the hybrid materials, compared to pure LDH parent materials, clearly indicate the presence of combustible nanocarbons in the hybrid catalysts. **As applied in previous publications [22], a simple rule-of-mixture analysis of the residue allows the estimation of the carbon content for both CuAl-LDH/GO and CoAl-LDH/GO (Table 1). In both samples a carbon content of about 3 wt% has been calculated.** This slightly lower carbon loading compared to the nominal GO weight fraction (5 wt%) is consistent with the loss of highly-oxidized, polyaromatic GO debris removed under the basic conditions of the materials synthesis and washing.

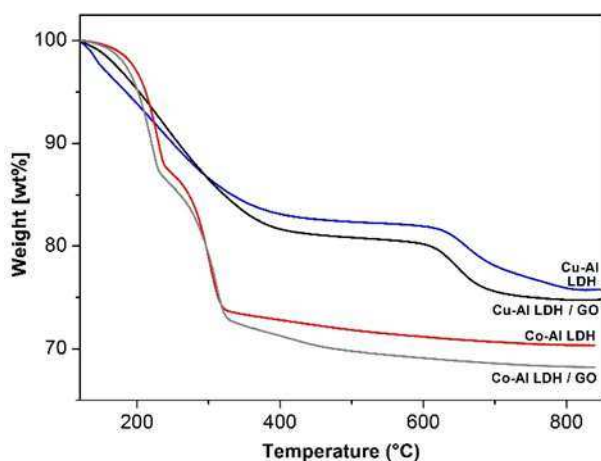


Fig. 3. TGA profiles (in air) of pure and GO-containing CuAl LDH and CoAl LDH.

XRD spectroscopy of the pure and hybrid catalyst powders (Figure 4) confirmed the crystallinity and crystal structure of the catalyst systems on the macroscopic scale. All catalyst systems showed reflections typical for LDH structures with no phase impurities apparent. Minor differences in the stacking of the double-hydroxide layers in the CuAl LDHs and CoAl LDHs give rise to different overall crystallographic symmetries, leading to the formation of hexagonal and rhombohedral hydroxalcalite-like structures, respectively [56]. In the hybrid catalysts, no diffraction features related to GO are observed due to the small loading fraction of GO, its relative disorder, and its high degree of exfoliation. Scherrer analysis of the LDH reflections at around  $2\theta=12^\circ$  indicate apparent crystal sizes in the c-direction (stacking direction of the LDH sheets) of around 43 nm for the CoAl-LDH but only 19 nm for the CuAl-LDH (Table 1). For the hybrid LDH/GO catalysts, the crystal domain sizes are virtually unchanged (Table 1), suggesting that the presence of small amounts of GO during catalyst synthesis has no significant impact on crystallinity.

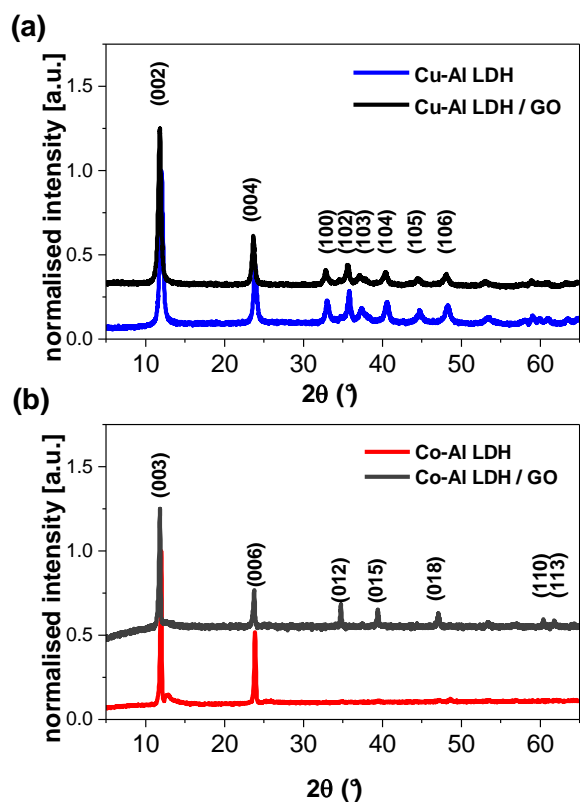


Fig. 4. XRD patterns of pure and GO-containing LDH catalysts: (a) Cu-Al LDH and Cu-Al LDH / GO; (b) Co-Al LDH and Co-Al LDH / GO.

Table 1. Materials characterisation data of the pure LDH and hybrid LDH/GO catalysts.

Sample	TGA (GO content, wt%)	BET ( $S_{\text{BET}}$ , $\text{m}^2 \cdot \text{gr}^{-1}$ )	<b>Nitrogen adsorption measurements</b> ( $V_{\text{Meso}}$ , $\text{cm}^3 \cdot \text{gr}^{-1}$ )	XRD ( $d_{003}$ , nm)
Cu-Al LDH	0	28.0	0.25	18.3
Cu-Al LDH / GO	3	44.3	0.25	19.5
Co-Al LDH	0	9.9	0.10	43.8
Co-Al LDH / GO	3	16.9	0.09	40.1

Liquid nitrogen adsorption measurements were conducted to investigate the textural properties of the pure and GO-containing LDH catalyst. All adsorption isotherms exhibited Type IV shape, typical for mesoporous adsorbents, consistent with previous reports on GO-supported nanocarbons. The specific surface area of CuAl-LDH is significantly larger than the one of the CoAl-LDH (Table 1), consistent with the differences in particle size observed by electron microscopy (Figure 2). Further, the BET data indicate considerable increases in specific surface area (about 100%) for both CuAl- and CoAl-LDH upon incorporation of only 3wt% GO (Table 1). While the total mesopore volumes remain unchanged upon GO incorporation (Table 1), the pore size distributions show a clear new

population of small pores (around 2-3 nm, Figure 5) in both CuAl-LDH/GO and CoAl-LD/GO, potentially due to small interstitial spaces created by the presence of GO nanosheets between individual LDH nanoparticles.

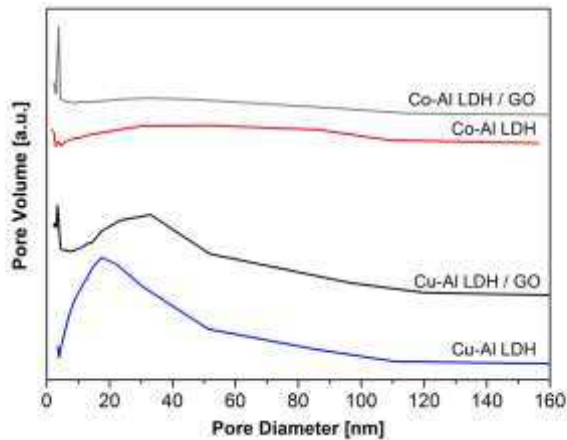


Fig. 5. Mesopore size distributions for pure and GO-containing Cu-Al and Co-Al LDHs, as derived from liquid nitrogen physisorption measurements.

The elemental composition of the catalysts in the bulk and on the surface was probed by electron dispersive spectroscopy (EDS) and X-ray photoelectron spectroscopy (XPS), respectively. Both methods confirmed the absence of sodium (a potential impurity from the catalyst synthesis that might affect catalyst performance). For the CoAl-LDH catalysts, the Co:Al ratio on the surface and in the bulk was found to be close to the nominal ratio of 2:1 as expected from the stoichiometry employed during synthesis. High-resolution XPS of the Co region exhibited the typical signature of Co (II) with no indication of other cobalt species. For the CuAl-LDHs, the molar Cu:Al ratio probed by EDS is close to the stoichiometric ratio 2:1. Determination of the elemental surface composition by XPS was not attempted for these systems as the significant overlap of the Cu and Al XPS peaks makes quantification unreliable. However, high resolution XPS of the Cu 2p peaks shows the typical profile for Cu (II). Deconvolution of the Cu 2p<sub>3/2</sub> photoelectron peak into two components at 933 eV and 934 eV respectively has been used to distinguish between separated, individual Cu (II) centres and clustered Cu (II) species, respectively [48]. Following this approach, copper is nearly exclusively (>90%) present as clustered species in the LDH materials produced. Both metals (II):Al (III) ratio and high-resolution XPS profile show no significant changes upon incorporation of GO for both Cu-Al and Co-Al LDH catalyst systems (ESI, Figure S1, S2, Table S1). These observation suggests that the presence of small concentrations of GO during LDH synthesis has no significant impact on the chemical composition of the materials.

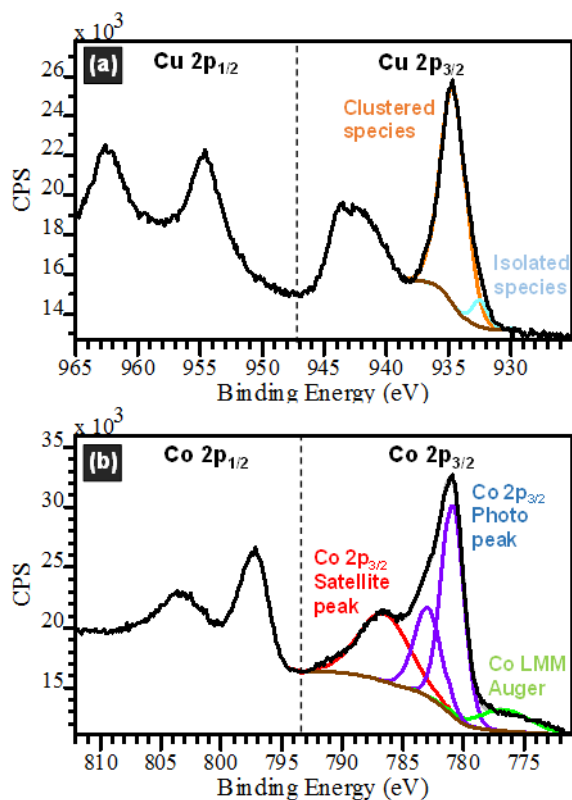


Fig. 6. High resolution XPS spectra of the metal (II) 2p region for (a) pure Cu-Al LDH, and (b) pure Co-Al LDH.

In order to test the reducibility of the materials, an important characteristic for performance in Ullmann coupling, temperature programmed reduction (TPR) measurements in  $H_2/Ar$  were conducted. The resulting TPR profiles were comparable to literature reports on TPR of copper and cobalt containing materials, respectively.

The pure CuAl LDH catalyst showed a two-component reduction peak at around  $255^\circ C$ , typical for the reduction of  $Cu^{2+}$ . It is noteworthy that no significant reduction events were observed at temperatures higher than  $300^\circ C$ , typical for the reduction of CuO clusters, suggesting that all  $Cu^{2+}$  species are well-incorporated into the brucite lattice of the LDH structure. The CuAl-LDH/GO catalyst exhibited an onset of reduction about  $15^\circ C$  earlier than the pure parent LDH. This earlier onset suggests slightly easier reduction, potentially related to the improved site accessibility in the LDH/GO hybrids, discussed above. The pure and hybrid CoAl-LDH catalysts showed broad reduction profiles at considerably higher temperatures ( $400-600^\circ C$ ), consistent with literature reports on the  $H_2$ -TPR characteristics of cobalt-containing materials [57]. For the CoAl-LDH/GO sample, a clear additional reduction peak at a lower temperature of around  $325^\circ C$  was observed, indicating again easier reduction of the GO-containing hybrid catalyst. The origin of this early reduction event is not clear, but could also be associated with improved site accessibility.

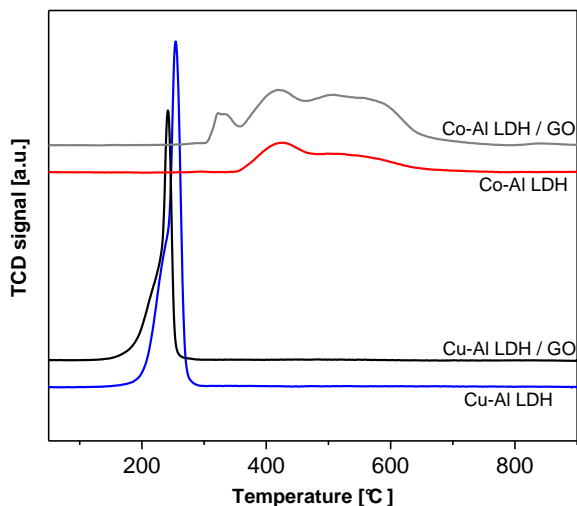


Fig. 7. H<sub>2</sub>-TPR profiles for pure and GO-containing Cu-Al and Co-Al LDHs.

The condensation of iodobenzene to biphenyl (Scheme 1) was chosen as the model reaction for the catalytic study of our CuAl LDH and CoAl LDH catalysts, due to its significance in organic synthesis [32]. All the catalysts showed substantial activity in short time (25 min), and a catalytic activity with a trend in the order CuAl LDH > CoAl LDH > CuAl LDH/GO > CoAl LDH/GO with respective reaction yields of 91, 88, 83, and 68%. Therefore, the best isolated biphenyl yields were achieved by Cu containing LDH catalysts. As a comparison, the catalytic activity of our catalyst and other Cu and Co catalysts reported in the literature over the Classic Ullmann Homocoupling Reaction to give unsubstituted biphenyls have been collected in Table 2.

Scheme 1: The classic Ullmann reaction for homocoupling of iodobenzene catalysed by Cu- and Co-containing LDH catalyst systems.

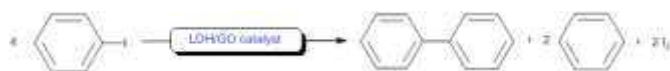


Table 2. Catalytic Yield of the biphenyl in the homocoupling of halo-benzene, Classic Ullmann Reaction (Scheme 1).

Entry	Benzene substitution	Cat.	mmol of halo-benzene	mmol of Cu or Co	Addition	time	T (°C)	Yield (%)	Ref.
Copper catalyst									
1	I	Commercial Cu	0.4	0.6		5 h	200	43	[47]
2	I	CuI-P(Et) <sub>3</sub>	10	20	Lithium naphthalide	24 h	85	66	[58]
3	I	Silica supported Cu	2	0.2	KF (base)	20 h	130	93	[37]
4	I	Sonochemically synthesised Cu	0.4	0.6		5 h	200	88	[47]
5	I	CuMgAILDH	2	*	Microwave	12 min	120	91	[48]
6	I	CuAl LDH	2	0.1 <sup>[1]</sup>		25 min	110	91	This work
7	I	CuAILDH/GO	2	0.1 <sup>[1]</sup>		25 min	110	83	This work
Cobalt catalyst									
8	Cl	CoBr <sub>2</sub>	1.5	0.5	Manganese dust (reducing agent)	7 h	50	32	[52]
9	Br	CoCl <sub>2</sub>	1	0.05	Grignard reagents and atmospheric oxygen	3 h	RT	81	[54]
10	MgCl	CoCl <sub>2</sub>	4	0.2	Synthetic air purge	30 min	0	86	[53]
11	I	CoAILDH	2	0.1 <sup>[1]</sup>		25 min	110	88	This work
12	I	CoAILDH/GO	2	0.1 <sup>[1]</sup>		25 min	110	68	This work

\* molarity data not available

[1] estimated by inductively coupled plasma atomic emission spectroscopy (ICP-AES).

It is of particular interest the catalytic performance shown by the CoAl LDH catalyst. As shown in Table 2, the catalytic yield for the homocoupling of iodobenzene is higher than the one reported in the literature (entries 9, 10 and 11 in Table 2). As mentioned in the introduction, there are less than 7 examples that show good yield (up to 65%) on homocoupling reactions using Co catalysts and those works were developed back in 1964. Recently, yields of up to 84% have been reported [52] for the same reaction using CoBr<sub>2</sub> but the substitution of phenyl groups by an electron withdrawing group was required resulting in the corresponding substituted biphenyl. When using halo-benzenes the only reported yield falls down to 32% (entry 8 in Table 2) and only shows better performance when using Grignard reagents (entry 9 in Table 2). Therefore, the unprecedented yields we report here (88%) open new horizons over the use of Co catalyst for Classic Ullmann Reactions. The reaction completion time has been also reduced considerably to 25 min. Comparable yield and completion time are only shown in entry 10 but however, the proposed reaction system requires a synthetic air purge and 0°C and therefore is less practicable if compared with the one proposed in the current study.

The unsupported CuAl LDH synthesised here (entry 6, Table 2) shows high conversion values (91%) but most importantly, the reaction completion time has been reduced by a factor of ten, specifically from 5 h to 25 min if we compare it with related works in literature (entry 4 in Table 2). Silica supported copper catalyst have shown yields of the same order of magnitude (entry 3 in Table 2). However, the reaction reported in this work is performed in the absence of base and the reaction completion time is forty times shorter. Indeed the reaction was completed in a very short reaction time and with a high yield using a conventional method as an alternative to previous work in our group using microwaves (entry 5 in Table 2) [48].

Cu and Co particle size can play an important role in the catalytic activity as reported by Gedanken [41]. As observed previously in our group [22] the precipitation of LDH onto graphene oxide leads to a smaller particle size if compared with the unsupported LDH due to a nucleation effect. The commercial copper (entry 1, Table 2) has been reported to have a particle size between 500 and 600 nm and shows 43 % conversion of iodobenzene to biphenyl. However, at the same experimental conditions, using sonochemically prepared copper (entry 4, Table 2) with particle size between 50-70 nm, the same authors show a conversion of about 88 %. The LDH platelets shown in the SEM and TEM pictures (Figures 1 and 2) have a lateral dimension of 100 nm and 8  $\mu\text{m}$  respectively for the Cu and Co LDH. XRD has shown also smaller crystal domain for the CuAlLDH than for the CoAlLDH hybrid. The particle size difference is reflected directly in a higher surface area shown by the CuAlLDH with a consequent higher exposition of the active sites to the reactants, and therefore showing higher catalytic activity if compared with the CoAlLDH. The finding supports the relation between particle size and catalytic activity; smaller particles provides a large amount of exposed active reaction centres improving the catalytic performance of the LDH itself. When introducing graphene oxide, the catalytic activity of the hybrids is lower in both catalyst, Cu and Co LDHs. Although the surface area of the dry hybrid is high (Table 1), when introducing the hybrid in DMSO for the catalytic test, a restacking of the GO layers can be provoked. The restacking of the GO layers can reduce the accessibility of the reactants to the active sites of the supported LDH. The same behaviour has been observed previously in our group. [22]

Nevertheless, the GO plays a critical role in the stability of the catalyst over reusability cycles; highly sought characteristic for industrial applications. The reusability of all the investigated catalysts was determined over five reaction cycles under optimized reaction conditions (Figure 8). It is shown from these results that after five regeneration cycles the GO-supported catalysts have better catalytic activity/selectivity and product's yield than the unsupported samples. It is remarkable the small loss of catalytic activity after 5 reaction cycles when the LDHs are supported on GO. The same behaviour has been observed previously in our group [22] proving that the GO gives the mechanical stability to stand the temperature switch during the cycles. In particular the stability of unsupported LDH is greatly improved by the addition of 3wt% of GO; after 5 cycles, the catalytic activity is about 1.4 times higher for the CuAl LDH/GO hybrid than for the pure LDH and nearly 2 times higher for the CoAl LDH/GO hybrid. In other words, the reaction yield of the biphenyl synthesis by GO supported Cu and Co catalysts drops slightly to approximately 70% of its initial value after the fifth cycle. Reusability studies over the same classic Ullmann reaction using other catalytic systems usually shows that after the fifth cycle, the yield decreases to 40 % of its initial value [46]. This significant result emphasizes the potential of LDH/GO hybrids containing low amounts of GO for catalytic applications. In this case, the mechanical properties of GO provide the stability to the hybrid. Moreover, the ease of separation and recovery of the catalyst leads to a lower amount of metal leached in the desired products, and makes possible the reuse of the catalyst for many cycles of production.

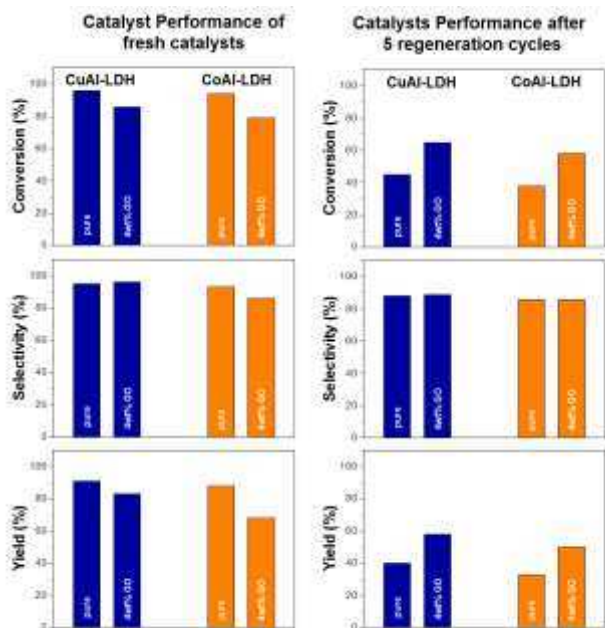


Fig 8. The catalytic properties of the investigated catalysts. Reaction conditions: Iodobenzene (1) (2.00 mmol), catalyst (0.25 g), DMSO (4 mL), reaction temperature; 110°C. <sup>b</sup> Isolated yields of biphenyl.

#### 4. Conclusions

Biaryl compounds are an important class of “building blocks” widely employed in polymer industries and pharmaceutical areas. Ullmann Classic Reaction is since 1901 [40], the main route to fabrication of unsubstituted biaryls. The Ullmann reaction was originally developed as a C–C coupling between aromatic halides induced by a transition metal. However, there are a series of drawbacks that makes the reaction industrially impractical. We report the synthesis and characterisation of CuAl layered double hydroxide (LDHs) and CoAl LDHs as new heterogeneous catalyst for the synthesis of biaryls by carbon-carbon coupling (Classic Ullmann Reaction). The CuAl-LDH and CoAl-LDH catalysts showed to be efficient, inexpensive solid heterogeneous catalysts that can catalyse the Ullmann coupling of aryls to biaryls in the absence of base, using practical reaction conditions, with short reaction times (25 min) and with a high yield. Indeed the obtained yields are among the highest reported for the same reaction using Cu and Co based catalysts (yields of 91% and 88 % for Cu and Co, respectively). The better performance can be related to the smaller particle size measured by transmission and scanning electron microscopy and therefore higher surface area, hence providing a large amount of exposed active reaction centres. The integration of high surface area 2D (graphene oxide GO) allows the dispersion of LDH over the surface due to geometric and charge compatibility between GO and LDH. However, GO’s poor network forming ability impacts in its overall catalytic activity. In the future, approaches to maintain an open GO structure as a support are likely to be beneficial, for example, by combinations of GO with materials such as carbon nanotubes [59] that provide an open framework structure. The resulting hybrid will provide a combination of active surface and network formation. However, the mechanical properties of GO allows an enhancement of the stability of the catalyst that can be separated and reused in the reaction several times with a loss of activity as low as 70 % of its initial value after 5 cycles. Moreover, this class of supported reagents can facilitate both the isolation and recycling of the catalyst by filtration, thus providing environmentally cleaner processes. Finally, LDH/GO hybrid structures are likely to be relevant to a wide variety of applications, including CO<sub>2</sub> sorption [22] and supercapacitors [60].

## 5. Acknowledgments

The authors are grateful to Prof M. S. P. Shaffer for advice and acknowledge financial support from the Deanship of Scientific Research at King Abdulaziz University (Grant D-1-434).

## 6. Notes and references

- [1] N. Sharma, H. Ojha, A. Bharadwaj, D.P. Pathak, R.K. Sharma, *RSC Advances*, 5 (2015) 53381-53403.
- [2] C. Li, M. Wei, D.G. Evans, X. Duan, *Small*, 10 (2014) 4469-4486.
- [3] S. Kannan, *Catal Surv Asia*, 10 (2006) 117-137.
- [4] S. Nishimura, A. Takagaki, K. Ebitani, *Green Chemistry*, 15 (2013) 2026-2042.
- [5] S.N. Basahel, S.A. Al-Thabaiti, K. Narasimharao, N.S. Ahmed, M. Mokhtar, *Journal of Nanoscience and Nanotechnology*, 14 (2014) 1931-1946.
- [6] Z.P. Xu, J. Zhang, M.O. Adebajo, H. Zhang, C. Zhou, *Applied Clay Science*, 53 (2011) 139-150.
- [7] G. Fan, F. Li, D.G. Evans, X. Duan, *Chemical Society Reviews*, 43 (2014) 7040-7066.
- [8] D.P. Debecker, E.M. Gaigneaux, G. Busca, *Chemistry – A European Journal*, 15 (2009) 3920-3935.
- [9] H. Li, D. Zhang, P. Maitarad, L. Shi, R. Gao, J. Zhang, W. Cao, *Chemical Communications*, 48 (2012) 10645-10647.
- [10] X. Du, D. Zhang, L. Shi, R. Gao, J. Zhang, *Nanoscale*, 5 (2013) 2659-2663.
- [11] X. Du, D. Zhang, R. Gao, L. Huang, L. Shi, J. Zhang, *Chemical Communications*, 49 (2013) 6770-6772.
- [12] E.M. Seftel, M. Niarchos, C. Mitropoulos, M. Mertens, E.F. Vansant, P. Cool, *Catalysis Today*, 252 (2015) 120-127.
- [13] R. Prakruthi, B.S. Jai Prakash, Y.S. Bhat, *Journal of Molecular Catalysis A: Chemical*, 408 (2015) 214-220.
- [14] F. Winter, V. Koot, A.J. van Dillen, J.W. Geus, K.P. de Jong, *Journal of Catalysis*, 236 (2005) 91-100.
- [15] M.-Q. Zhao, Q. Zhang, J.-Q. Huang, F. Wei, *Advanced Functional Materials*, 22 (2012) 675-694.
- [16] J. Wang, G. Fan, H. Wang, F. Li, *Industrial & Engineering Chemistry Research*, 50 (2011) 13717-13726.
- [17] J. Wang, G. Fan, F. Li, *Catalysis Science & Technology*, 3 (2013) 982-991.
- [18] M.G. Álvarez, A.M. Frey, J.H. Bitter, A.M. Segarra, K.P. de Jong, F. Medina, *Applied Catalysis B: Environmental*, 134–135 (2013) 231-237.
- [19] H. Wang, X. Xiang, F. Li, *Journal of Materials Chemistry*, 20 (2010) 3944-3952.
- [20] M. Gong, Y. Li, H. Wang, Y. Liang, J.Z. Wu, J. Zhou, J. Wang, T. Regier, F. Wei, H. Dai, *Journal of the American Chemical Society*, 135 (2013) 8452-8455.
- [21] A. Celaya-Sanfiz, N. Morales-Vega, M. De Marco, D. Iruretagoyena, M. Mokhtar, S.M. Bawaked, S.N. Basahel, S.A. Al-Thabaiti, A.O. Alyoubi, M.S.P. Shaffer, *Journal of Molecular Catalysis A: Chemical*, 398 (2015) 50-57.
- [22] A. Garcia-Gallastegui, D. Iruretagoyena, V. Gouvea, M. Mokhtar, A.M. Asiri, S.N. Basahel, S.A. Al-Thabaiti, A.O. Alyoubi, D. Chadwick, M.S.P. Shaffer, *Chemistry of Materials*, 24 (2012) 4531-4539.
- [23] R. Xie, G. Fan, Q. Ma, L. Yang, F. Li, *Journal of Materials Chemistry A*, 2 (2014) 7880-7889.
- [24] J.P. Finet, A. Fedorov, S. Combes, G. Boyer, *Current Organic Chemistry*, 6 (2002) 597-626.
- [25] S.V. Ley, A.W. Thomas, *Angewandte Chemie International Edition*, 42 (2003) 5400-5449.
- [26] K. Kunz, U. Scholz, D. Ganzer, *Synlett*, 2003 (2003) 2428-2439.
- [27] I.P. Beletskaya, A.V. Cheprakov, *Coordination Chemistry Reviews*, 248 (2004) 2337-2364.
- [28] R. Frlan, D. Kikelj, *Synthesis*, 2006 (2006) 2271-2285.
- [29] Q. Fan, J.M. Gottfried, J. Zhu, *Accounts of Chemical Research*, 48 (2015) 2484-2494.
- [30] C. Sambigioglio, S.P. Marsden, A.J. Blacker, P.C. McGowan, *Chemical Society Reviews*, 43 (2014) 3525-3550.
- [31] H. Lin, D. Sun, *Organic Preparations and Procedures International*, 45 (2013) 341-394.
- [32] D.A. Horton, G.T. Bourne, M.L. Smythe, *Chemical Reviews*, 103 (2003) 893-930.
- [33] F. Monnier, M. Taillefer, *Angewandte Chemie International Edition*, 47 (2008) 3096-3099.

- [34] B. Sreedhar, R. Arundhathi, P.L. Reddy, M.L. Kantam, *The Journal of Organic Chemistry*, 74 (2009) 7951-7954.
- [35] T. Wang, J.A. Love, *Synthesis*, 2007 (2007) 2237-2239.
- [36] T. Miao, L. Wang, *Synthesis*, 2008 (2008) 363-368.
- [37] Q. Wu, L. Wang, *Synthesis*, 2008 (2008) 2007-2012.
- [38] J. Zhang, Z. Zhang, Y. Wang, X. Zheng, Z. Wang, *European Journal of Organic Chemistry*, 2008 (2008) 5112-5116.
- [39] R. Zhang, J. Liu, S. Wang, J. Niu, C. Xia, W. Sun, *ChemCatChem*, 3 (2011) 146-149.
- [40] F. Ullmann, J. Bielecki, *Berichte der deutschen chemischen Gesellschaft*, 34 (1901) 2174-2185.
- [41] H.-J. Cristau, P.P. Cellier, S. Hamada, J.-F. Spindler, M. Taillefer, *Organic Letters*, 6 (2004) 913-916.
- [42] A. Ouali, J.-F. Spindler, H.-J. Cristau, M. Taillefer, *Advanced Synthesis & Catalysis*, 348 (2006) 499-505.
- [43] G. Li, C. Liu, Y. Lei, R. Jin, *Chemical Communications*, 48 (2012) 12005-12007.
- [44] D.A. Culkin, J.F. Hartwig, *Journal of the American Chemical Society*, 123 (2001) 5816-5817.
- [45] Y. Wan, J. Chen, D. Zhang, H. Li, *Journal of Molecular Catalysis A: Chemical*, 258 (2006) 89-94.
- [46] W. Yao, W.-J. Gong, H.-X. Li, F.-L. Li, J. Gao, J.-P. Lang, *Dalton Transactions*, 43 (2014) 15752-15759.
- [47] N.A. Dhas, C.P. Raj, A. Gedanken, *Chemistry of Materials*, 10 (1998) 1446-1452.
- [48] K. Narasimharao, E. Al-Sabban, T.S. Saleh, A.G. Gallastegui, A.C. Sanfiz, S. Basahel, S. Al-Thabaiti, A. Alyoubi, A. Obaid, M. Mokhtar, *Journal of Molecular Catalysis A: Chemical*, 379 (2013) 152-162.
- [49] G. Cahiez, A. Moyeux, *Chemical Reviews*, 110 (2010) 1435-1462.
- [50] M. Amatore, C. Gosmini, *Angewandte Chemie International Edition*, 47 (2008) 2089-2092.
- [51] P. Gomes, H. Fillon, C. Gosmini, E. Labbé, J. Périchon, *Tetrahedron*, 58 (2002) 8417-8424.
- [52] A. Moncomble, P. Le Floch, C. Gosmini, *Chemistry – A European Journal*, 15 (2009) 4770-4774.
- [53] M. Mayer, W.M. Czaplik, A. Jacobi von Wangelin, *Synlett*, 2009 (2009) 2919-2923.
- [54] S.-Y. Chen, J. Zhang, Y.-H. Li, J. Wen, S.-Q. Bian, X.-Q. Yu, *Tetrahedron Letters*, 50 (2009) 6795-6797.
- [55] Z. Liu, R. Ma, M. Osada, N. Iyi, Y. Ebina, K. Takada, T. Sasaki, *Journal of the American Chemical Society*, 128 (2006) 4872-4880.
- [56] F. Cavani, F. Trifirò, A. Vaccari, *Catalysis Today*, 11 (1991) 173-301.
- [57] G. Jacobs, Y. Ji, B. Davis, D. C. Cronauer, A. J. Kropf, C. L. Marshall, *Applied Catalysis A. General*, 333 (2007) 177-191.
- [58] G.W. Ebert, R.D. Rieke, *The Journal of Organic Chemistry*, 53 (1988) 4482-4488.
- [59] A. Garcia-Gallastegui, D. Iruretagoyena, M. Mokhtar, A.M. Asiri, S.N. Basahel, S.A. Al-Thabaiti, A.O. Alyoubi, D. Chadwick, M.S.P. Shaffer, *Journal of Materials Chemistry*, 22 (2012) 13932-13940.
- [60] L. Wang, D. Wang, X.Y. Dong, Z.J. Zhang, X.F. Pei, X.J. Chen, B. Chen, J. Jin, *Chemical Communications*, 47 (2011) 3556-3558.